Applied Physics Express 6 (2013) 062301
http://dx.doi.org/10.7567/APEX.6.062301

Enhancement of Conversion Efficiency of Cu_2ZnSnS_4 Thin Film Solar Cells by Improvement of Sulfurization Conditions

Tatsuo Fukano*, Shin Tajima, and Tadayoshi Ito

Toyota Central Research and Development Laboratories Inc., Nagakute, Aichi 480-1192, Japan
E-mail: e0987@mosk.tytlabs.co.jp

Received April 17, 2013; accepted May 20, 2013; published online June 7, 2013

To enhance the conversion efficiency of Cu_2ZnSnS_4 (CZTS) thin film solar cells prepared by the sulfurization method, we investigated the formation process of the CZTS thin film. The holding temperature of the sulfurization was 580 °C. This study showed that the spreading resistance (SR) of the CZTS layer strongly depends on the holding time of the sulfurization. At the intermediate holding time (~30 min), the SR of the CZTS layer came to a minimum, and the efficiency of the CZTS solar cell came to a maximum. A 7.6% efficiency CZTS solar cell without a high-resistance buffer layer and an antireflection coating was fabricated. © 2013 The Japan Society of Applied Physics

Cu_2ZnSnS_4 (CZTS) and $Cu_2ZnSn(S_xSe_{1-x})$ (CZTSSe) have been studied as p-type semiconductors for absorber layers of thin film solar cells. In particular, CZTS has the suitable optical bandgap energy of 1.4–1.5 eV;[1,2] in addition, all the constituents of CZTS are abundant and non-toxic. After the CZTS solar cell with a conversion efficiency exceeding 6% was reported,[3] the efficiencies of CZTSSe and CZTS solar cells have rapidly improved.[4–11] Solar cells based on CZTSSe absorber layers can be fabricated by various methods such as a solution process using hydrazine,[5] a solution process using water,[8] and a vacuum deposition process,[9,10] and all have high efficiencies. In contrast, the absorber layers of high-efficiency CZTS solar cells are predominantly fabricated by sulfurization of the precursors by a vacuum deposition process[3,6,7] and an open atmosphere type chemical vapor deposition method.[11] The wide variety of formation processes for CZTSSe layers compared to CZTS layers may reflect that it is more difficult to form CZTS layers for high-efficiency solar cells. Thus, in the case of CZTS solar cells, it is considered that understanding the formation process of the CZTS absorber layer prepared by the sulfurization method is especially helpful in enhancing the efficiency. The formation processes of CZTS layers from various monolayer or multilayer precursors under constant sulfur pressure have been studied.[12–14] Specifically, the crystal structure of the grains, the sub-phase materials, and the composition of the CZTS layers have been the major subjects of research. However, it is well known that the optimizations of the crystal structure and the composition of the CZTS layers are not always sufficient to fabricate solar cells with high conversion efficiency. In this study, we investigated the change in electrical characteristics of the CZTS absorber layers during the sulfurization process in addition to the crystal structure and the composition of the CZTS layers. Then, based on an understanding of the sulfurization process, a CZTS thin film solar cell with a conversion efficiency exceeding 7% was fabricated.

Mo electrode layers 1 μm in thickness were formed on alkali-glass substrates by sputter deposition. Four-layered CZTS precursors 700–800 nm in thickness were deposited by RF magnetron sputtering using Cu, Sn, and ZnS as the targets. The (alkali-glass/Mo/)ZnS/Sn/Cu/ZnS precursor structure was adopted to fabricate the solar cells. The two ZnS layers were of equal thickness. The CZTS absorber layers were formed by sulfurizing the CZTS precursors. The sulfurization process was carried out by heating the precursors to 580 °C and keeping them for a given holding time in 20 vol % H_2S balanced with N_2. The heating and cooling rates were 5 and −5 °C/min, respectively. The pressure was maintained at atmospheric pressure. To determine the optimum holding time, we investigated as follows. The precursors were heated to 580 °C and held for 10–60 min. The composition of the CZTS absorber layers on the Mo electrode layers was estimated using X-ray fluorescence (XRF) analysis. The atomic ratios of Cu/(Zn + Sn), Cu/Sn, and Zn/Sn were 0.80–0.90, 1.65–1.85, and 1.02–1.10, respectively. Their crystal structures were confirmed by the kesterite-type using X-ray diffraction (XRD) analysis. Both the atomic ratios and the crystal structures were independent of the holding time. Solar cells with the CZTS absorber layers sulfurized for different holding times were fabricated. The cell structure did not include a high-resistance buffer layer and an antireflection coating. CdS buffer layers 70–100 nm in thickness were chemically grown on the CZTS absorber layers by the chemical bath deposition (CBD) method. Ga-doped ZnO window layers 100–200 nm in thickness and Al comb-shaped electrodes were formed by sputter deposition and electron beam deposition, respectively. Then, the current–voltage (I–V) characteristics of the solar cells were measured using a solar simulator under air mass 1.5 and 100 mW/cm^2 illumination. The conversion efficiencies (η) of the solar cells with the CZTS absorber layers sulfurized for 10, 30, and 60 min were 4.8, 5.6, and 1.5%, respectively.

An intermediate holding time (30 min) was necessary to form the CZTS absorber layer for the high-performance solar cell. However, the difference in the conversion efficiencies of the CZTS solar cells made with the different holding times of sulfurization at 580 °C was not accounted for by the macroscopic composition and crystal structure of the CZTS absorber layers. We focused on the electrical property of the CZTS absorber layers to understand the mechanism that caused the variation in conversion efficiency due to different sulfurization holding times. The cross-sectional surfaces of the CZTS solar cells made with different holding times were analyzed by scanning spreading resistance microscopy (SSRM). Figure 1 shows the time-course of the cross-sectional spreading resistance (SR) images of the CZTS solar cells. At the short holding time (10 min), the SR of the whole CZTS absorber layer is low. This is probably due to the high carrier density induced by

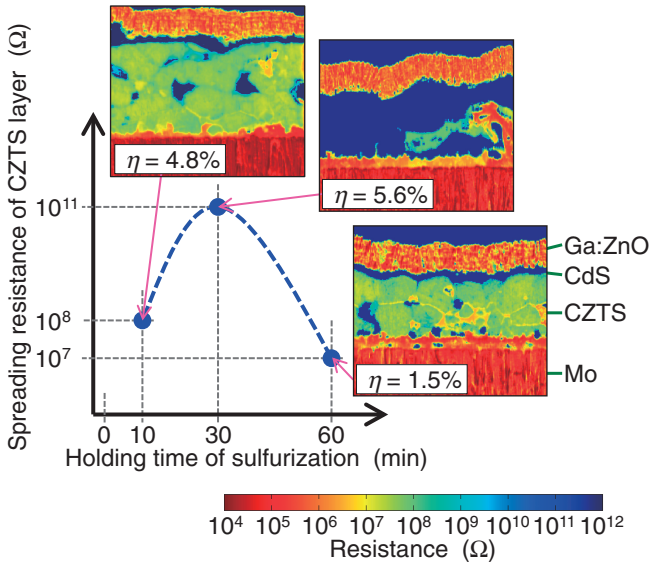

Fig. 1. Time-course (10–60 min) of cross-sectional SR images of CZTS solar cells by SSRM during sulfurization at 580 °C. At 30 min, the SR of the whole CZTS absorber layer becomes as large as the SR of the CdS buffer layer.

various point defects that remain in the CZTS crystal grains because of insufficient heat quantity. At the intermediate holding time (30 min), the SR of the whole CZTS absorber layer becomes as high as the SR of the CdS buffer layer. The increase in the SR is probably caused by a decrease in the amount of point defects due to stabilization of the CZTS crystal grains. At the long holding time (60 min), the SR of the whole CZTS absorber layer becomes low, and the lowest SR areas are formed at the CZTS grain boundaries. The low SR of the CZTS grains is probably caused by an increase in the carrier density induced by point defects in the CZTS crystals. The increased point defects are supposedly Cu substitutions at Zn sites, which are dominant acceptors in p-type CZTS crystals.[15] The low SR at the CZTS grain boundaries is probably caused by the formation of low-resistance materials, supposedly induced by the diffusion of excess alkali metal ions from the alkali-glass substrate to the CZTS absorber layer through the Mo electrode layer.

Moreover, by changing the precursor structure from the four-layered precursor with (alkali-glass/Mo/)ZnS/Sn/Cu/ZnS to the three-layered precursor with (alkali-glass/Mo/)ZnS/Sn/Cu, we fabricated a CZTS thin film solar cell with high efficiency. The atomic ratios of Cu/(Zn + Sn), Cu/Sn, and Zn/Sn of the CZTS absorber layers sulfurized at 580 °C for 30 min were within the abovementioned range. The tendency of the time-course of the SR of the CZTS solar cell was not affected by the change in precursor structure. The cross-sectional scanning transmission electron microscope (STEM) bright-field image of the solar cell is shown in Fig. 2. The CZTS absorber layer is made up of densely packed large grains with low surface roughness. The grain size is larger in the three-layered precursor than in the four-layered precursor (Fig. 1). In the three-layered precursor, the grains are as large as the thickness of the CZTS layer. Figure 3 presents the *I–V* characteristics of the best performance CZTS solar cell measured at the National Institute of Advanced Industrial Science and Technology

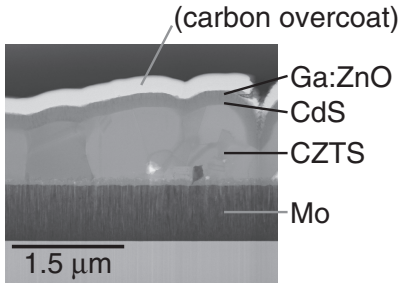

Fig. 2. Cross-sectional STEM bright-field image of the CZTS solar cell. The CZTS absorber layer is made up of densely packed large grains.

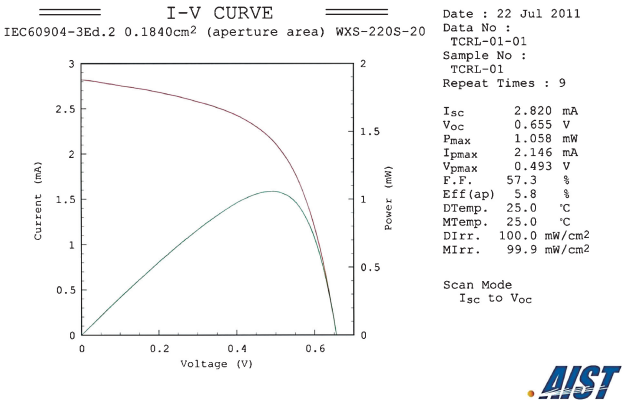

Fig. 3. *I–V* characteristics of the best performance CZTS solar cell measured at AIST.

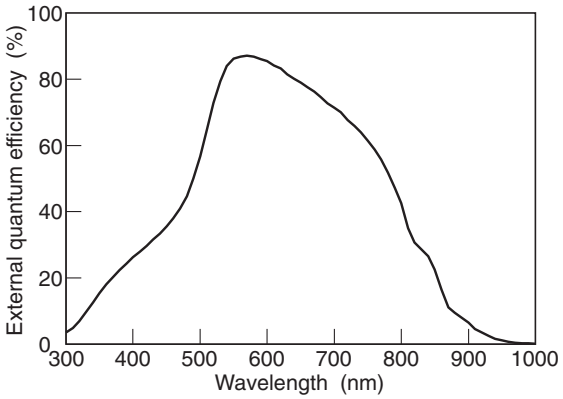

Fig. 4. EQE spectrum curve of the best performance CZTS solar cell. The decline of the EQE spectrum in the 400–540 nm wavelength range is caused by optical absorption of the CdS buffer layer.

(AIST). The conversion efficiency (η) in the aperture area (0.184 cm^2), the open-circuit voltage (V_{oc}), the short-circuit current density (J_{sc}) in the aperture area, and the filling factor (FF) are 5.8%, 655 mV, 15.33 mA/cm^2, and 57.3%, respectively. Since the active area of the best CZTS solar cell is 0.140 cm^2, η, and J_{sc} in the active area are 7.6% and 20.14 mA/cm^2, respectively. Figure 4 shows the external quantum efficiency (EQE) spectrum curve of the best CZTS solar cell. The EQE spectrum is higher than 80% in the spectral region from 540 to 640 nm. The decline of the EQE spectrum in the 400–540 nm wavelength range is caused by optical absorption of the CdS buffer layer. The EQE is lower

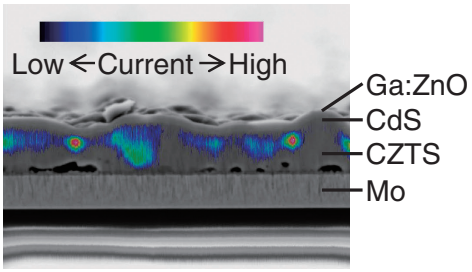

Fig. 5. Image of EBIC signal on the cross-sectional SEM image of the best performance CZTS solar cell. The EBIC signal presents a patchy pattern.

than 80% in the 640–800 nm wavelength range. The image of an electron beam induced current (EBIC) signal on the cross-sectional scanning electron microscope (SEM) image of the CZTS solar cell is shown in Fig. 5. The EBIC signal presents a patchy pattern on the CZTS absorber layer around the interface between the CZTS absorber layer and the CdS buffer layer. The uniformity of the power generation region is still low.

In conclusion, we investigated the formation process of CZTS absorber layers by sulfurization using 20 vol % H_2S balanced with N_2. Our study showed that the spreading resistance (SR) of the CZTS absorber layer strongly depends on the holding time of the sulfurization. After identifying the optimum holding time, we succeeded in fabricating a CZTS thin film solar cell with a conversion efficiency of 7.6%.

Acknowledgments We would like to thank T. Eguchi and T. Maki, Toyota Industries Corporation, for their supporting this investigation. We wish to thank Dr. Y. Hishikawa, National Institute of Advanced Industrial Science and Technology, for the precise measurements of *I–V* characteristics. We appreciate Dr. T. Motohiro and Dr. K. Higuchi, Toyota Central R&D Labs. Inc., for fruitful discussions.

1) H. Katagiri: Thin Solid Films **480–481** (2005) 426.
2) K. Jimbo, R. Kimura, T. Kamimura, S. Yamada, W. S. Maw, H. Araki, K. Oishi, and H. Katagiri: Thin Solid Films **515** (2007) 5997.
3) H. Katagiri, K. Jimbo, S. Yamada, T. Kamimura, W. S. Maw, T. Fukano, T. Ito, and T. Motohiro: Appl. Phys. Express **1** (2008) 041201.
4) D. A. R. Barkhouse, O. Gunawan, T. Gokmen, T. K. Todorov, and D. B. Mitzi: Prog. Photovoltaics **20** (2012) 6.
5) T. K. Todorov, J. Tang, S. Bag, O. Gunawan, T. Gokmen, Y. Zhu, and D. B. Mitzi: Adv. Energy Mater. (in press) [DOI: 10.1002/aenm.201200348].
6) K. Wang, O. Gunawan, T. Todorov, B. Shin, S. J. Chey, N. A. Bojarczuk, D. Mitzi, and S. Guha: Appl. Phys. Lett. **97** (2010) 143508.
7) H. Sugimoto, H. Hiroi, N. Sakai, S. Muraoka, and T. Katou: Proc. 38th IEEE Photovoltaic Specialists Conf., 2012, 002997.
8) Y. Cao, M. S. Denny, Jr., J. V. Casper, W. E. Farneth, Q. Gio, A. S. Ionkin, L. K. Johnson, M. Lu, I. Malajovich, D. Radu, H. D. Rosenfeld, K. R. Choudhury, and W. Wu: J. Am. Chem. Soc. (in press) [DOI: 10.1021/ja.3057985].
9) B. Shin, Y. Zhu, N. A. Bojarczuk, S. Jay Chey, and S. Guha: Appl. Phys. Lett. **101** (2012) 053903.
10) G. Brammertz, M. Buffière, Y. Mevel, Y. Ren, A. E. Zaghi, N. Lenaers, Y. Mols, C. Koeble, J. Vleugels, M. Meuris, and J. Poortmans: Appl. Phys. Lett. **102** (2013) 013902.
11) T. Washio, T. Shinji, S. Tajima, T. Fukano, T. Motohiro, K. Jimbo, and H. Katagiri: J. Mater. Chem. **22** (2012) 4021.
12) R. Schurr, A. Hölzing, S. Jost, R. Hock, T. Voß, J. Schulze, A. Kirbs, A. Ennaoui, M. Lux-Steiner, A. Weber, I. Kötschau, and H.-W. Schock: Thin Solid Films **517** (2009) 2465.
13) A. Weber, R. Mainz, and H. W. Schock: J. Appl. Phys. **107** (2010) 013516.
14) T. Eguchi, T. Maki, S. Tajima, T. Ito, and T. Fukano: PVSEC-21 Tech. Dig., 2011, 4D-3P-24.
15) A. Nagoya, R. Asahi, R. Wahl, and G. Kresse: Phys. Rev. B **81** (2010) 113202.